

## LA-UR-18-20086

Approved for public release; distribution is unlimited.

Title: Testing ALE code FLAG with analytical self-similar solutions of 2D magnetized implosion.

Author(s): Bereznyak, Andrey  
Gianakon, Thomas Arthur  
Rousculp, Christopher L.  
Cooley, James Hamilton  
Giuliani, John

Intended for: Report

Issued: 2018-01-04

---

**Disclaimer:**

Los Alamos National Laboratory, an affirmative action/equal opportunity employer, is operated by the Los Alamos National Security, LLC for the National Nuclear Security Administration of the U.S. Department of Energy under contract DE-AC52-06NA25396. By approving this article, the publisher recognizes that the U.S. Government retains nonexclusive, royalty-free license to publish or reproduce the published form of this contribution, or to allow others to do so, for U.S. Government purposes. Los Alamos National Laboratory requests that the publisher identify this article as work performed under the auspices of the U.S. Department of Energy. Los Alamos National Laboratory strongly supports academic freedom and a researcher's right to publish; as an institution, however, the Laboratory does not endorse the viewpoint of a publication or guarantee its technical correctness.

# Testing ALE code FLAG with analytical self-similar solutions of 2D magnetized implosion.

*A. Beresnyak(1), T. Gianakon(2), C. Rousculp(2), J.H. Cooley(2), J. Giuliani(1)*  
1-NRL; 2-LANL

## Introduction

FLAG is an Arbitrary Lagrange Eulerian (ALE) code developed at Los Alamos National Laboratory as part of Advanced Simulation and Computing (ASC) program. Resistive Magneto-hydrodynamics (MHD) is under active development within the code for the purpose of modeling experiments on the Sandia Z-machine, modeling and design of flux compression generators (FCG), modeling of FCG loads used for proposed EOS experiments to be funded by the LANL Science Campaigns, and modeling of exploding wire configurations. The intent of this LANL/NRL collaboration is to use the analytic MHD test problems developed by NRL in Ref. [1] to facilitate verification and improvement of the ideal MHD package within FLAG and for NRL to explore usage of FLAG for their applications. One topic of interest for NRL is plasma devices with complex boundaries, such as dense plasma focus (DPF). Calculations can be improved by using the ability of FLAG to generate complex meshes and deal with plasma/vacuum interface. NRL is also particularly interested in the stability of Problem 3 since many codes have had limited success reproducing the results due to either numerical or actual instability. As a result of this collaboration, improvements in the formulation and implementation of the magnetic stress tensor ( $\mathbf{J} \times \mathbf{B}$  forces in the momentum equation) have been made as well as improvements to the advection (high order, low order, FCT) of the MHD state variables. Confidence in the implementation of MHD in FLAG code has increased for user applications due to this collaboration.

Velikovich et al., [1] have published a self-similar 2D solution of a collapsing magnetized z-pinch, extension of the classical Noh problem of infinite-Mach number collapse to MHD. We refer this below as "Problem 1". These involve constant implosion velocity, as in classic Noh, but density depending on radius as  $r^{2\beta}$  and magnetic field depending on radius as  $r^\beta$ . Infinite number of solutions exists for different betas and gas constants  $\gamma$ . The above authors also constructed two other solutions that are designated as "Problem 2" and "Problem 3". Problem 1 has zero out-of plane field  $B_z$  and only an azimuthal field  $B_\phi$ . Problem 2 has a stiffer equation of state with  $\gamma=2$  and both  $B_z$  and  $B_\phi$ . Problem 3 also has both  $B_z$  and  $B_\phi$  but a very soft equation of state with  $\gamma=1.1$  and high Alfvénic Mach number ( $v/v_A$ ). The self-similar solutions were constructed to have a shock speed the same for all three cases and equal to  $10^7$  cm/s. We typically compare numerics with analytical solution at 30ns when the shock is at  $r=0.3$ cm.

FLAG has flexibility regarding the geometry of the mesh (1D, 2D axially symmetric, 2D Cartesian, and 3D Cartesian) as well as the actual mesh. Furthermore, the mesh can move with the fluid (Lagrange), or be fixed in space (Eulerian), or be intermediate between the two (ALE). In addition to being able to run in 2D Cartesian geometry with ALE, FLAG can be run in 2D R-Z cylindrical geometry as well. This is referred to in the input as “axis2” option. The Lagrangian, staggered-grid hydro scheme present in FLAG utilizes a discretization scheme that converts the cylindrical differential operators into Cartesian form by appropriate choice of the point masses. This is often referred to as an area-weight scheme and is discussed in depth elsewhere (see Refs. [2], [3]). The magnetic  $\mathbf{J} \times \mathbf{B}$  forces contribute to the momentum equation as the divergence of a stress tensor quantity in a similar fashion as solid mechanics. In ideal MHD, magnetic flux is constrained to move with the Lagrange fluid. Additionally, results from the Godunoff based finite volume code ATHENA code are presented.

In this round of testing, three types of grid/geometry were considered (see Fig. 1) : 1) “fixed- grid” is a regular rectangular grid in 2D Cartesian with Eulerian mesh motion, similar to fixed grids used in Eulerian codes; 2) “box-grid” is 2D Cartesian having a box in the center and  $r$ - $\phi$  grid on the outside, with Lagrange mesh motion; and 3) “axis2-grid” is a regular Cartesian mesh in 2D axially symmetric geometry with Lagrange mesh motion. The resolution of fixed grid was constant while the resolution for box-grid and axis2-grid was increasing during the simulation due to the Lagrange fluid motion, in a sort-of “natural grid refinement.” For “fixed-grid” and for “box-grid”  $B_z$  is oriented out of the plane of the 2D mesh and  $B_\phi$  is in the plane of the mesh. For “axis2-grid”  $B_z$  is oriented in the plane of the mesh and  $B_\phi$  is normal to the plane of the mesh.

Section 2 presents a qualitative and quantitative comparison of results for the three problems from both FLAG and ATHENA. The intent is to look for symmetry breaking and mesh imprinting since the mesh is in general not aligned with the radial inward flow. The section includes a detailed comparison with the analytic solution. Concluding remarks are in Section 3.

## Results

In successful runs that we refer to below resolution was:

	dx , cm	0.3cm/dx
<b>Fixed grid</b>		
Prob1, Prob2	0.0093	32
Prob3	0.025	12
<b>Box grid at t=30ns, center</b>		
Prob1, Prob2	0.0067	45
Prob3	0.048	6
<b>Axis2 grid</b>		
Prob1, Prob2	0.06,0.03	50,100
Prob 3, Uniform	0.06	151
Prob 3, Ratio	$\alpha=0.95$	50

Problem 1 is observed to have artifacts in the upstream (shocked) domain with both FLAG fixed-grid and FLAG box-grid as illustrated in Figure 2. The solution for Problem 2 looked normal, axisymmetric, having no numerical artifacts as illustrated in Figure 3. Problem 3 was highly non-axisymmetric with strong  $m=4$  perturbation due to the grid, as illustrated in Figure 4. At higher resolution, FLAG simulations of Problem 3 developed numerical instabilities, both upstream and downstream of the shock. This typically ended the simulation because of the time step constraints. All three problems were run with Axis2-grid in FLAG and the results appear credible. Detailed comparisons follow in Figures 5-8 for Problem1, Figures 9-12 for Problem 2, and Figures 13-16 for Problem 3 with FLAG fixed-grid, FLAG box-grid, FLAG axis2-grid, and ATHENA.

### Magnetic Noh Problem 1:

Figure 5 shows the results for FLAG with fixed-grid and Figure 6 for FLAG with box-grid at  $t = 0.3 \mu s$ . Both solutions have the qualitatively correct behavior, though significant noise is apparent in the solution. The suspicion is that this is symptomatic of the non-flow aligned mesh and the first order shock capturing hydro. The magnetic fields are also computed through a least-squares from the underlying magnetic flux through “surface facets”. This may introduce numerical noise that might be expected to be reduced under mesh refinement. However, the

FLAG results were unexpectedly unstable under mesh refinement for this problem. This may be caused by poor time-step controls for MHD in FLAG. Figure 7 shows the results for FLAG with axis2-grid under mesh refinement. The solutions here appear to be converging to the analytic solution. Finally, Figure 8 shows the solutions from ATHENA, which appear to have excellent agreement with the analytic solution.

### **Magnetic Noh Problem 2:**

This problem includes a z-component of magnetic field along with different initial conditions from Problem 1. Figure 9 and Figure 10 presents the solution at  $t = 0.3 \mu\text{s}$  results for FLAG fixed-grid and FLAG box-grid respectively. Problem 2 was the easiest for FLAG to deal with in the box-grid configuration. An artifact at the origin for  $B_z$  and pressure is unclear.  $B_z$  is just threading the domain more or less uniformly and the origin is not special for  $B_z$ . Convergence is clearly not complete -- especially at the origin and at the shock. Figure 11 shows the results of a similar set of calculations for FLAG axis2-grid Only  $N_{\text{cells}} = 50$  and 100 (red and green) have been computed. The solutions show convergence to the analytic under radial mesh refinement and the shock is again in the correct location,  $r = 0.3 \text{ cm}$ . FLAG axis2-grid appears to also have the greatest error in the pressure at the origin. This may be related to the well-known errors in calculating strong shock solutions (Ref.[4]). Further investigation is warranted since the sound speed  $\sim \sqrt{p/\rho}$  in cell next to the origin limits the time step for the over the duration of the calculation which leads to single-processor run times in excess of five hours for  $N_{\text{cells}} = 100$ . This can be partially remedied by moving to ratio zoning or equal mass zoning though the impact on the MHD solution is presently unknown. Finally, Figure 12 shows the solutions from ATHENA, which again appear to have excellent agreement with the analytic solution.

### **Magnetic Noh Problem 3:**

Problem 3 is similar to Problem 2, but has a very soft equation of state with  $\gamma=1.1$  and high Alfvénic Mach number ( $v/v_A$ ). Figure 13 and Figure 14 present the solution at  $t = 0.3 \mu\text{s}$  results for FLAG fixed-grid and FLAG box-grid respectively. These solutions were unstable and comparison with the analytic solutions was largely meaningless. Surprisingly, the FLAG-axis2 solutions presented in Figure 15 agree nominally well with the analytic solution. If Problem 3 is actually physically unstable, this might be expected in that axis-2 is effectively 1 dimensional and would not be prone to seeding of instabilities due to misalignment of flow and field. Fixed-grid and box-grid would be prone to the seeding of instabilities. A converged accurate solution was achieved with ATHENA as presented in Figure 16. Athena was able to achieve accurate solution with some degree of grid-scale viscosity and resistivity. The ideal version of the code gave relative errors of order  $\sim 0.3$  which were only slowly decreasing with increasing resolution. Solution convergence for

Problem 3 for ideal version of Athena is presented on Fig. 19. The convergence is evidentially very slow. When Athena is additionally stabilized with viscosity and magnetic diffusivity ( $Pr_m = 1$ ,  $v = v_m \sim dx$ ) the solution is more accurate (Fig. 20).

## Conclusion

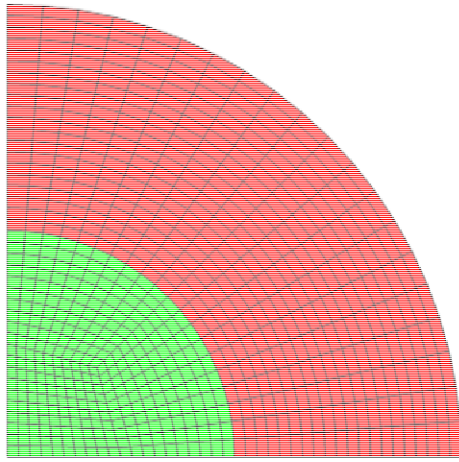
In the course of running the first and second magnetic Noh problems, bugs in coding were exposed that caused the results to deviate from the analytic solution. The coding has been corrected. Furthermore, at the time of these simulations, only a high order advection scheme had been implemented. Such schemes are known to be problematic in the presence of shocks. A low order scheme has since been implemented (in 2D) and a plan is underway to combine the low order and high order solutions into an FCT approach. The advection scheme may also need improvement to maintain local Divergence  $B = 0$ .

In the current configuration the FLAG solution becomes numerically unstable at sufficiently high resolution for all three test problems. Timestep controls for the MHD package may be the culprit. ATHENA solutions are in very good agreement with the analytic solutions, though Problem 3 required the introduction of additional dissipation. Concern exists that Problem 3 may be physically unstable. Problems 1 and 2 with FLAG qualitatively match, but more work is needed to reach accurate, quickly converging solutions. Problem 3 seems to present a serious problem for FLAG.

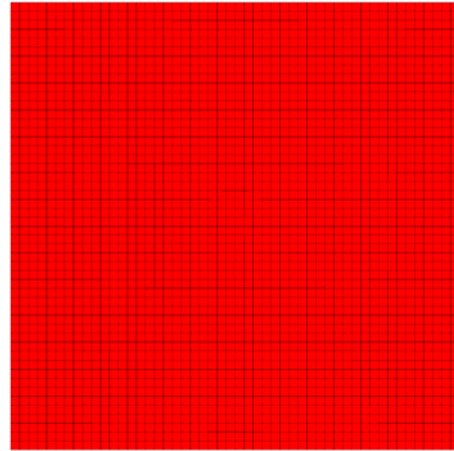
The goal of this collaboration was to provide a mechanism to verify the MHD implementation in FLAG and improve the FLAG MHD packages as need to meet broader LANL institutional goals. These three Magnetic Noh problems are proving immensely useful.

## References

- [1] A. L. Velikovich, J. L. Giuliani, S. T. Zalesak, J. W. Thornhill, and T. A. Gardiner, "Exact self-similar solutions for the magnetized Noh Z pinch problem", *Phys. of Plasmas*, **19**, 012707:1–12 (2012). doi:10.1063/1.3678213)
- [2] E. J. Caramana and P. P. Walen, "Numerical Preservation of Symmetry Properties of Continuum Problems", *J. Comp. Phys.*, **141**, 174–198 (1998).
- [3] M. Kenamond, M. Bement, and M. Shashkov, "Compatible, total energy conserving and symmetry preserving arbitrary Lagrangian–Eulerian hydrodynamics in 2D rz – Cylindrical coordinates", *J. Comp. Phys.*, **268**, 154–185 (2014).
- [4] W. F. Noh, "Errors for calculations of strong shocks using an artificial viscosity and an artificial heat flux", *J. Comp. Phys.*, **72**, 78–120 (1978).



(a)



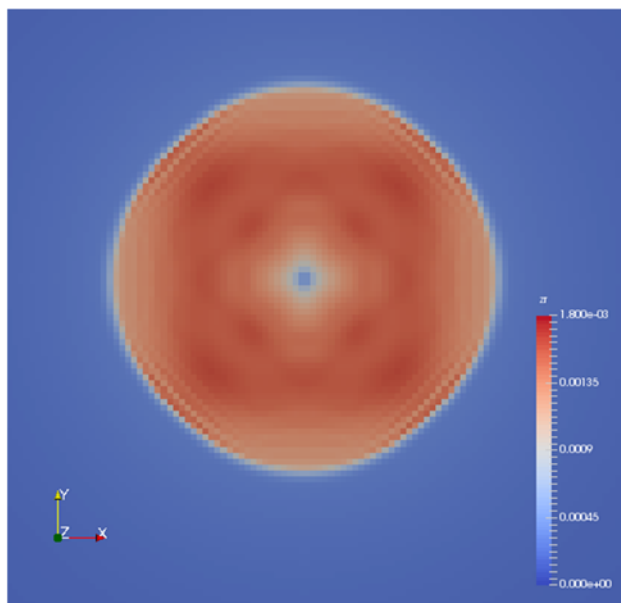
(b)



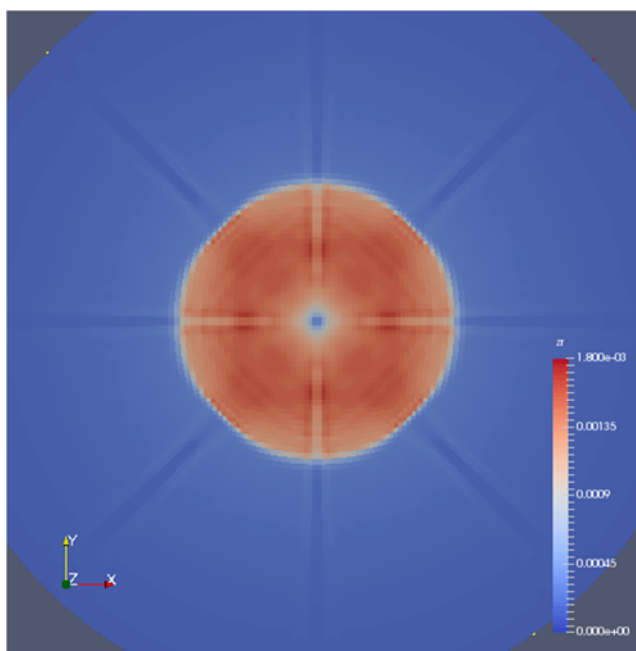
(c)

**Figure 1. Initial mesh for box-grid (a), fixed-grid (b), and axis2-grid (c). In both box-grid and fixed-grid the  $B_z$  field is out of the plane and the  $B_\phi$  field is in the plane of the mesh. Here, (a) is only the upper quarter octant, though the solution is on the full cross-section. Axis-2 has  $B_z$  field is in the plane of the mesh and  $B_\phi$  field is normal to the plane of the mesh. For Axis-2, Problem 3 both uniform and ratio zone meshes were considered. Ratio zoning was advantageous due to the low density at the center of the problem.**



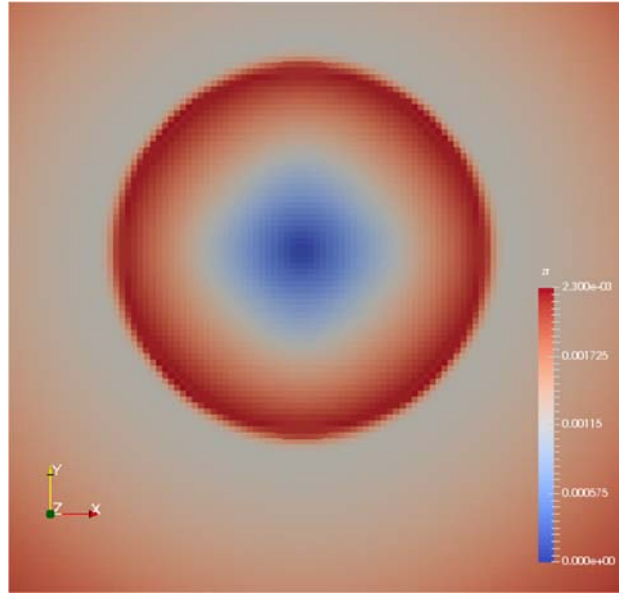


(a)

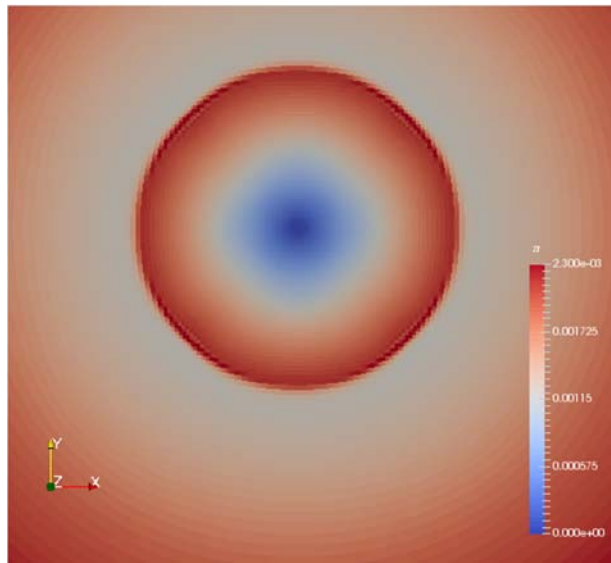


(b)

**Figure 2. Density profile for Problem 1 at  $t = 0.3 \mu\text{s}$  with Fixed-Grid (a) and Box-Grid (b) is observed to be symmetric. Some  $m=4$  and  $m=8$  artifacts are observed internal to the shock.**

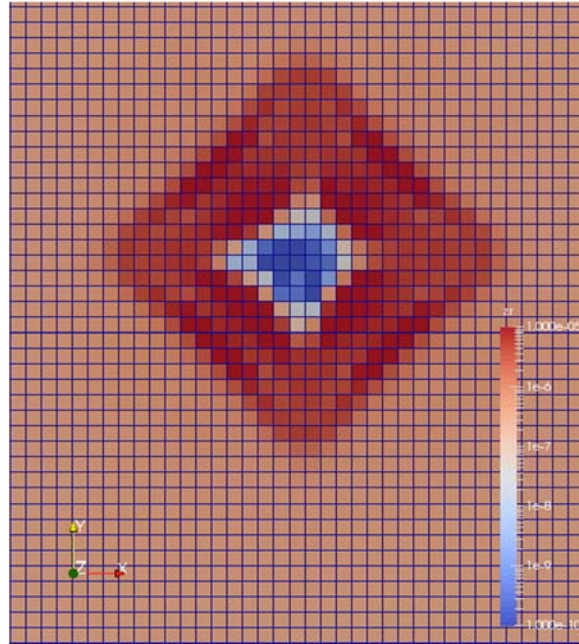


(a)

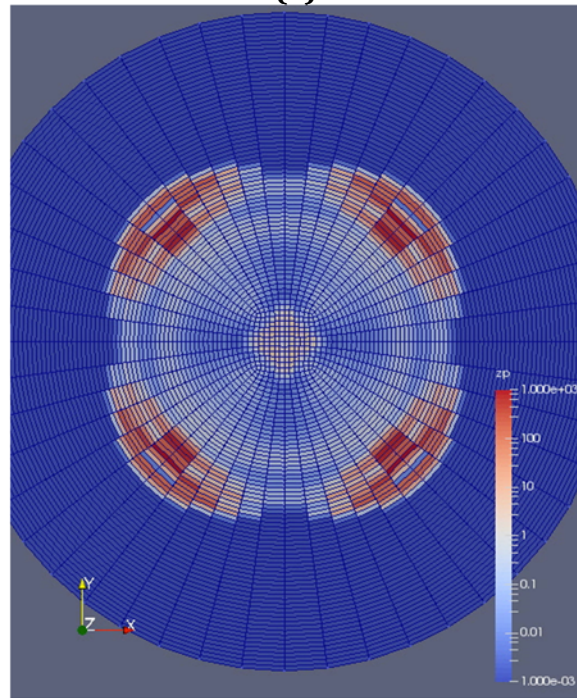


(b)

Figure 3. Density profile for Problem 2 at  $t = 0.3 \mu\text{s}$  fixed-grid (a) and box-grid (b) has no observable mesh imprinting.



(a)



(b)

**Figure 4. Pressure profiles for Problem 3 at  $t = 0.3 \mu\text{s}$  with fixed-grid (a) and box-grid (b). Numerical instability develops inside (a) and outside (b) of the domain of shocked gas.**

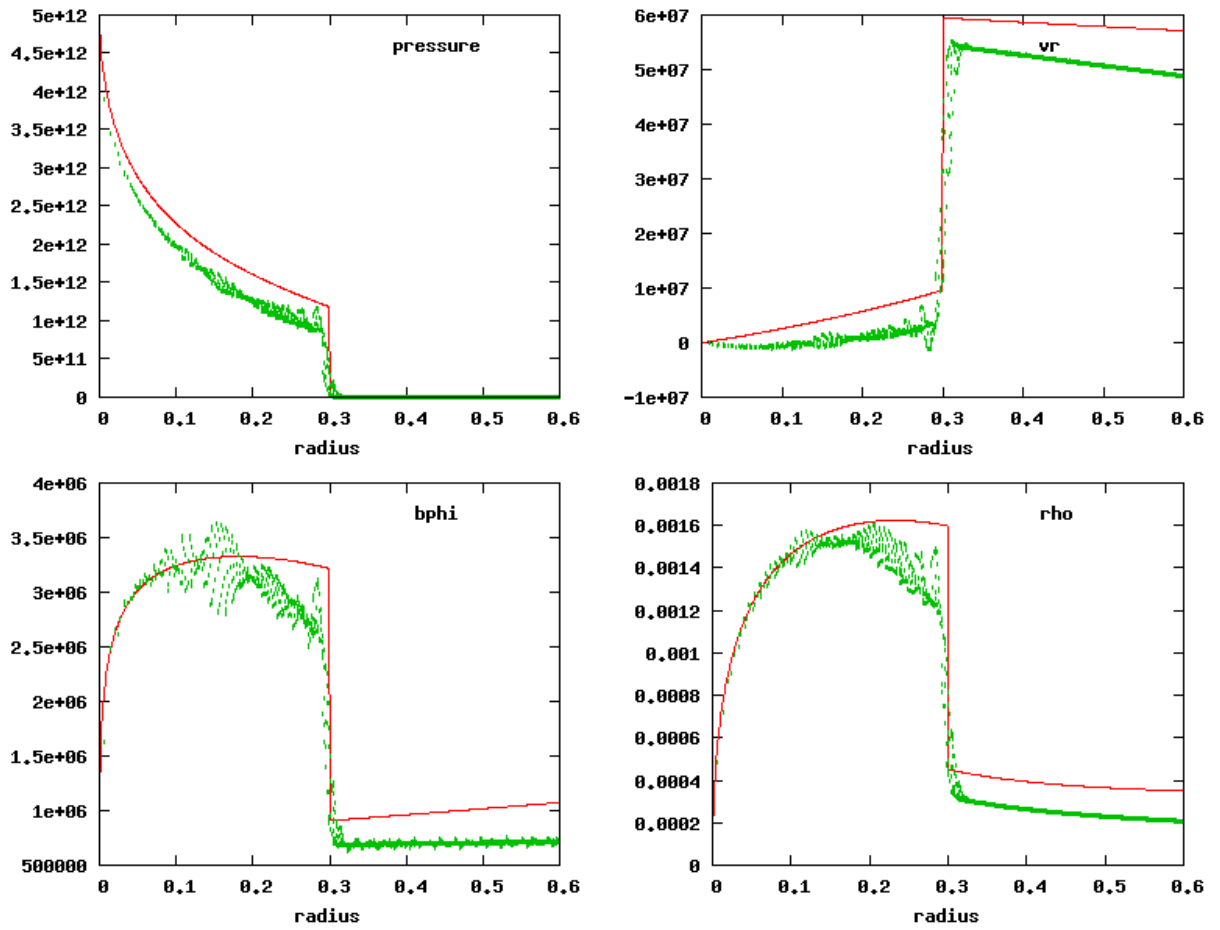


**Figure 5. Problem 1 with FLAG fixed-grid (red - analytical, green - numerical) has a qualitatively correct behavior.**

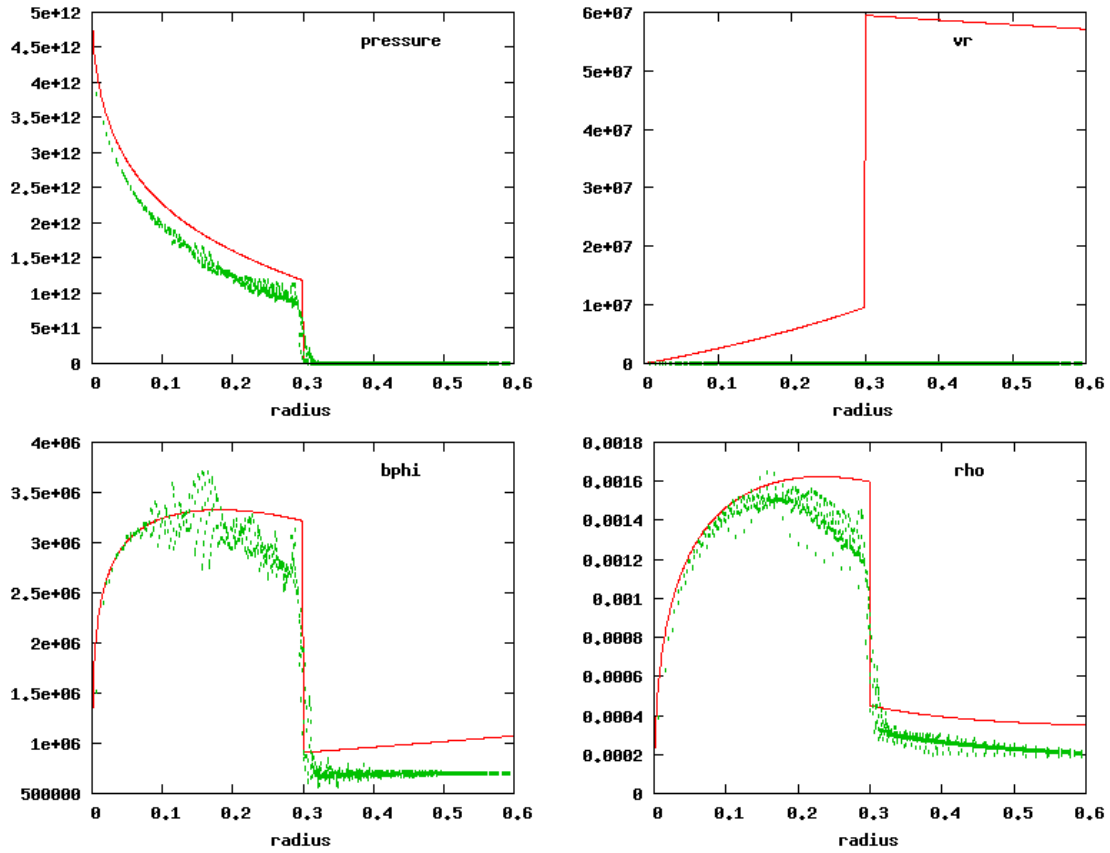


**Figure 6. Problem 1 with FLAG box-grid (red - analytical, green - numerical) has a qualitatively correct behavior. A bug was identified in the output of velocity in the upper quadrant that has since been resolved.**

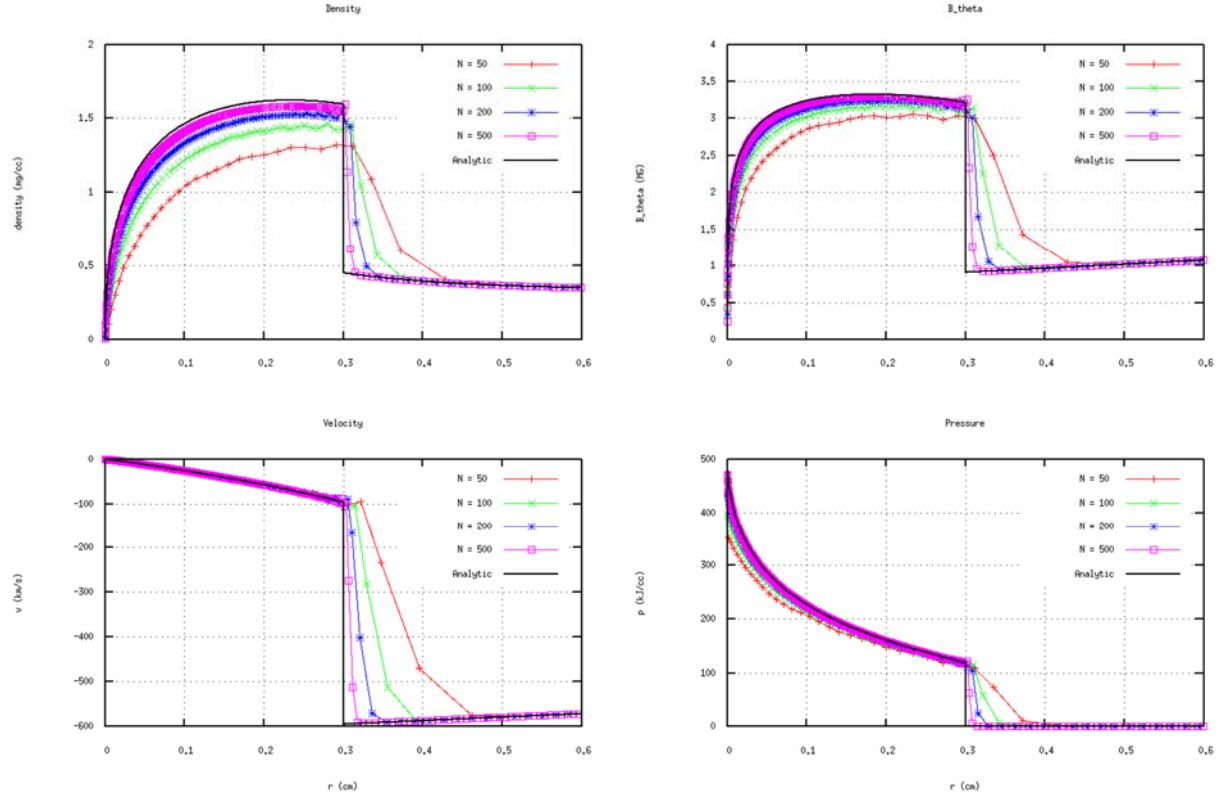


**Figure 7. Problem 1 with FLAG Axis2-grid (cylindrical) results at  $t = 0.3 \mu\text{s}$  under radial mesh refinement converges to the analytic solution. A series of calculations at successively higher, initial radial mesh resolution are run.  $N_{\text{cells}} = 50, 100, 200, 500$  are evenly distributed over  $0.0 < r < 3.0$ . The code is run in pure Lagrangian mode without ALE. By inspection, the solution appears to be converging to the analytic solution for the quantities, density, velocity, magnetic field, and pressure and the shock location is nominally located at  $r = 0.3$  cm.**

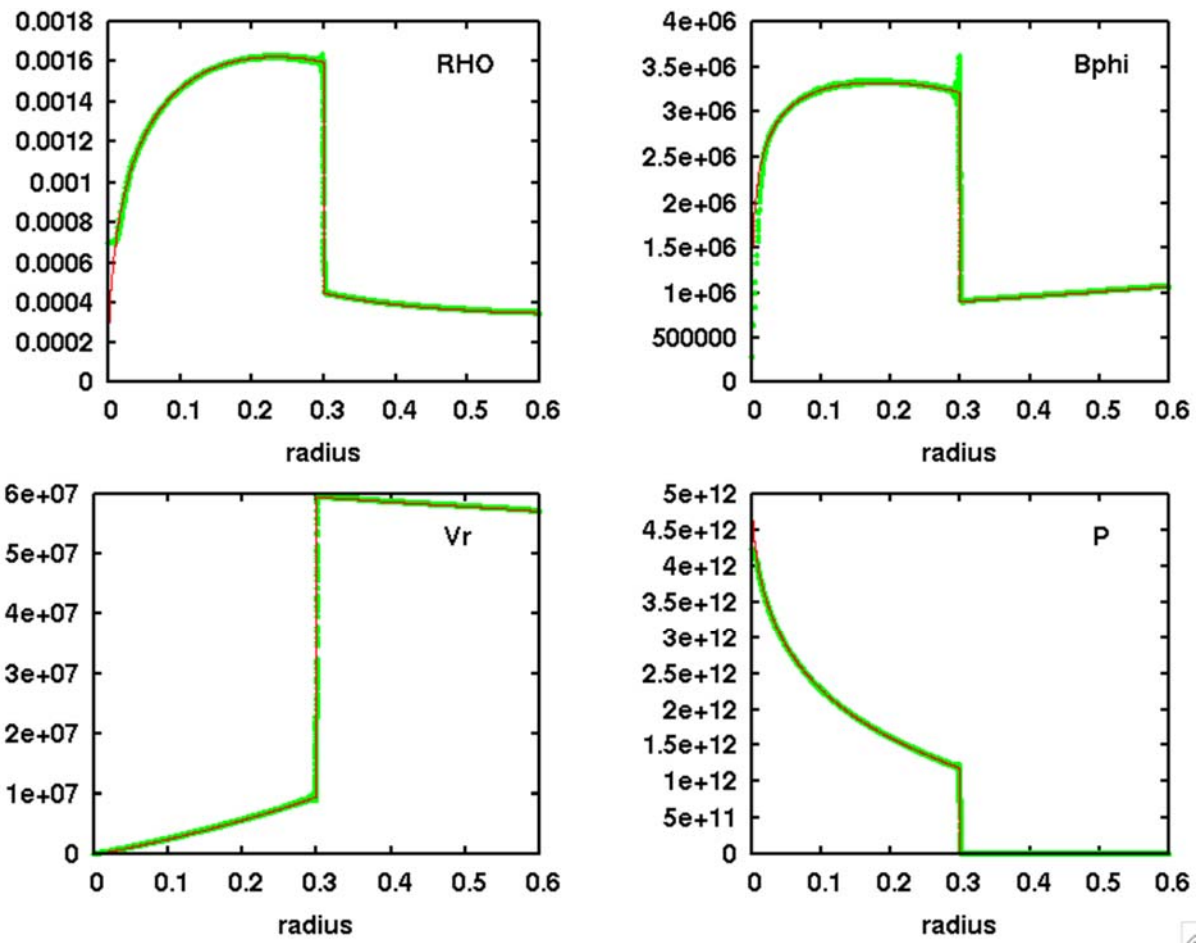


Figure 8. Problem 1 with ATHENA (fixed-grid) agrees with analytic solution.

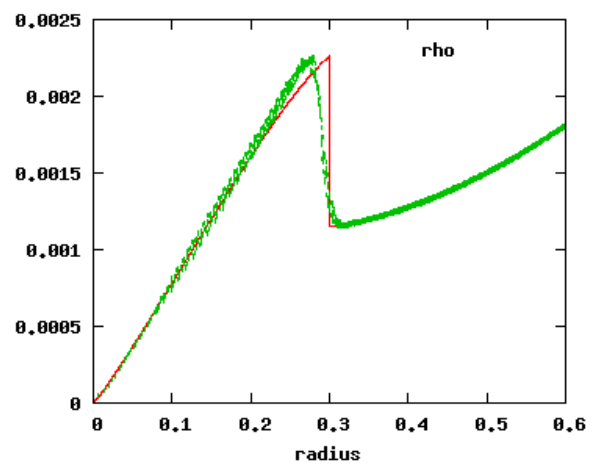
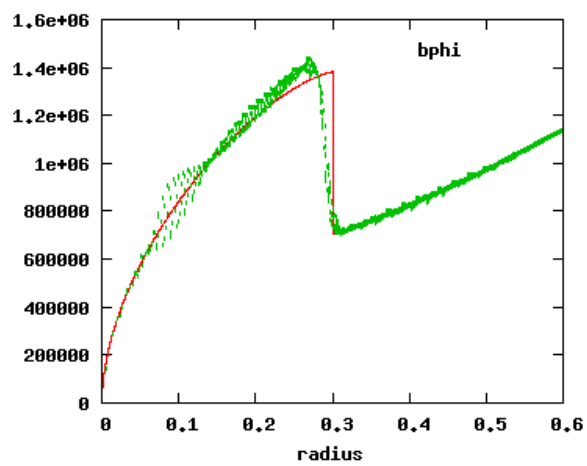
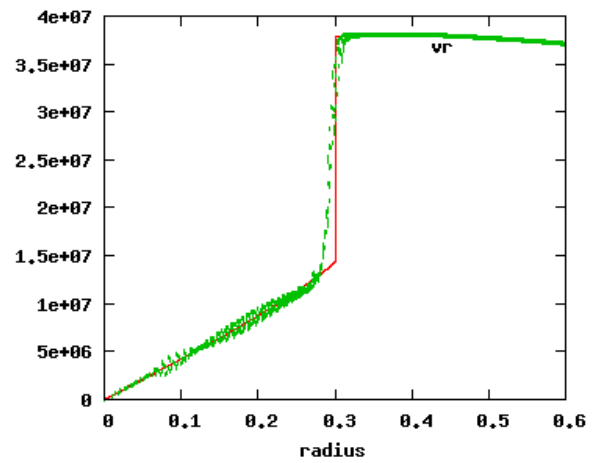
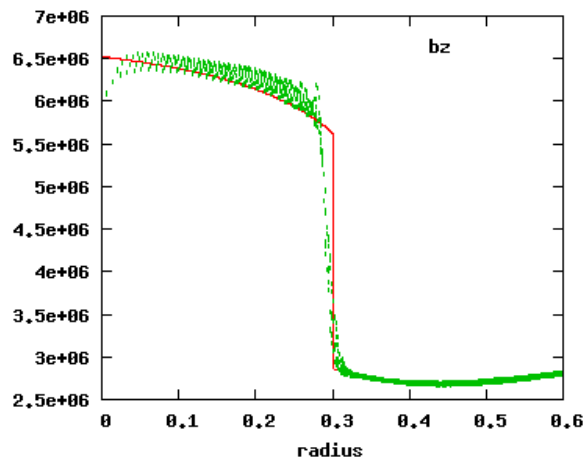
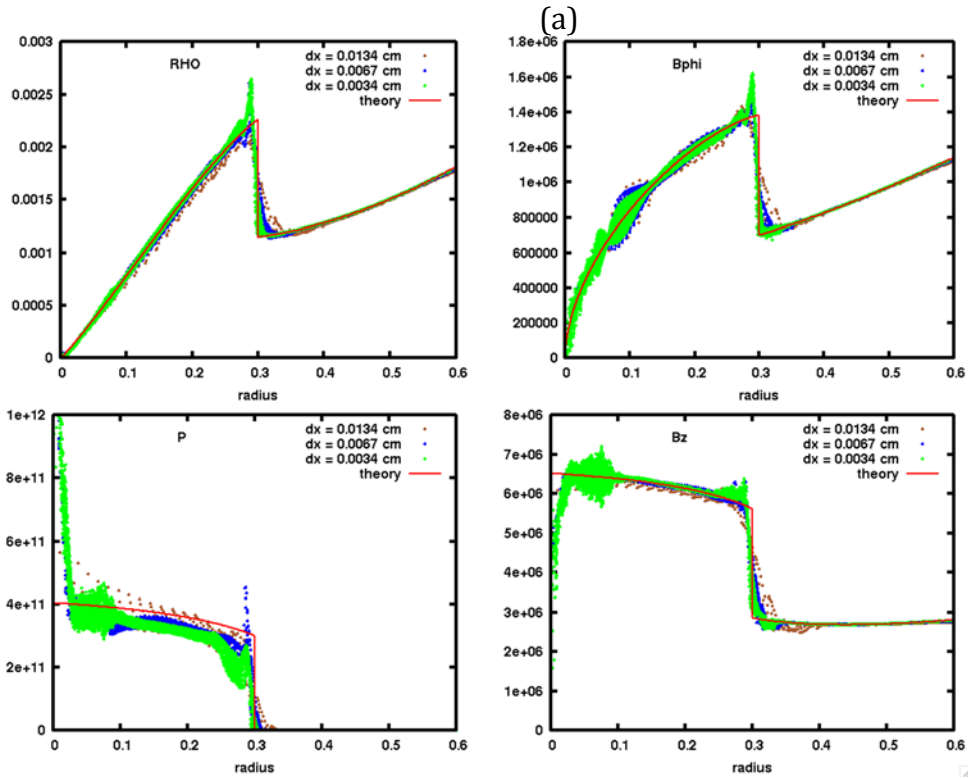
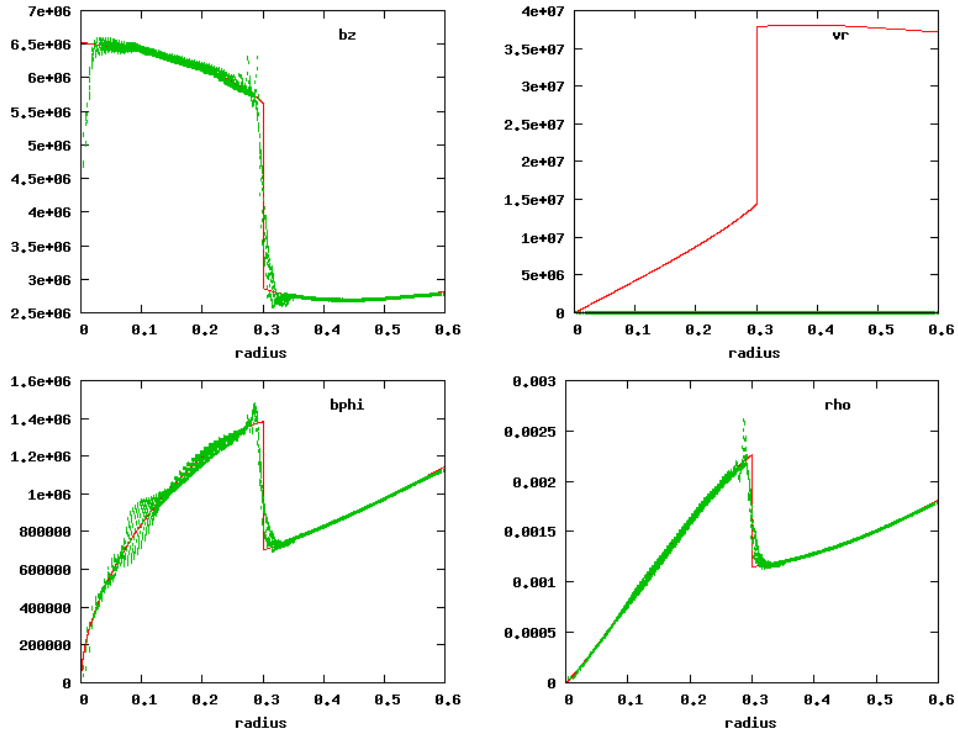


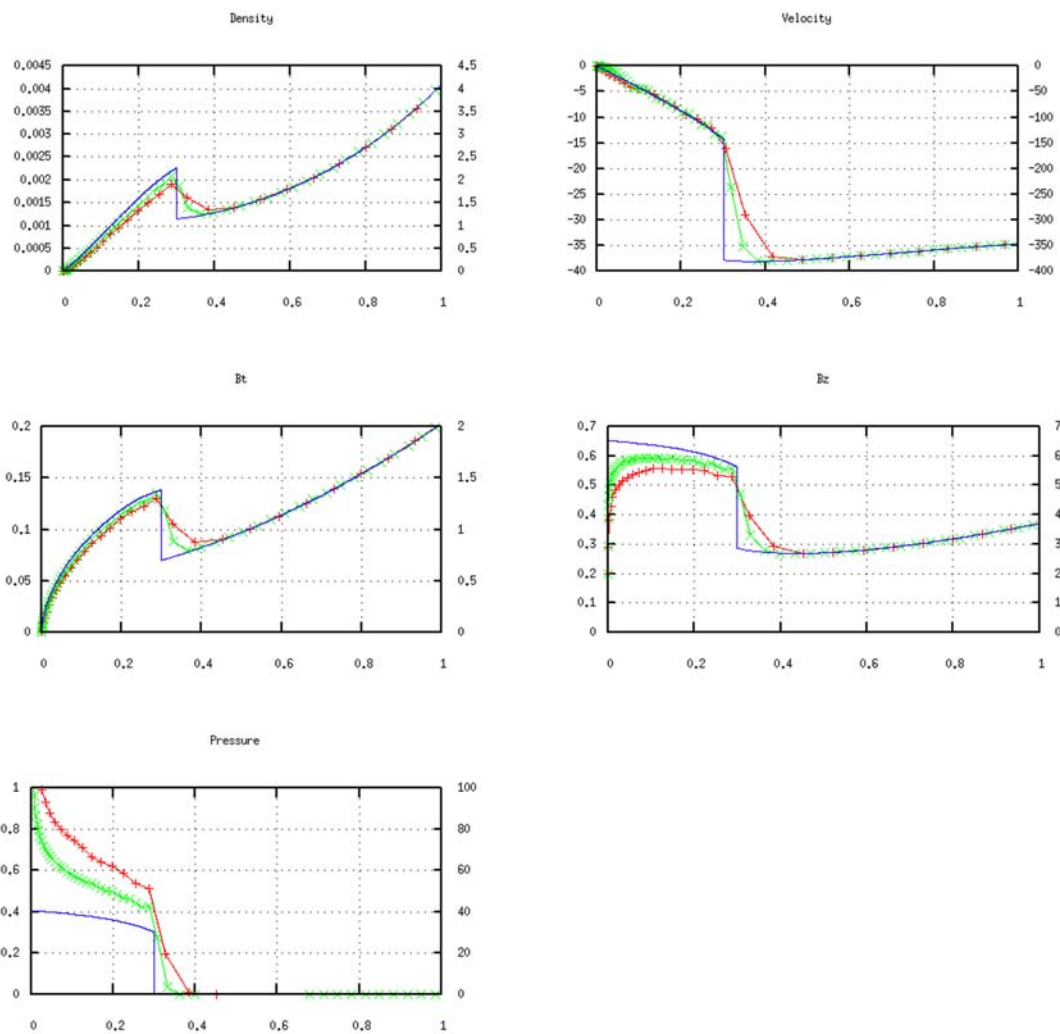
Figure 9. Fixed grid, Problem 2.





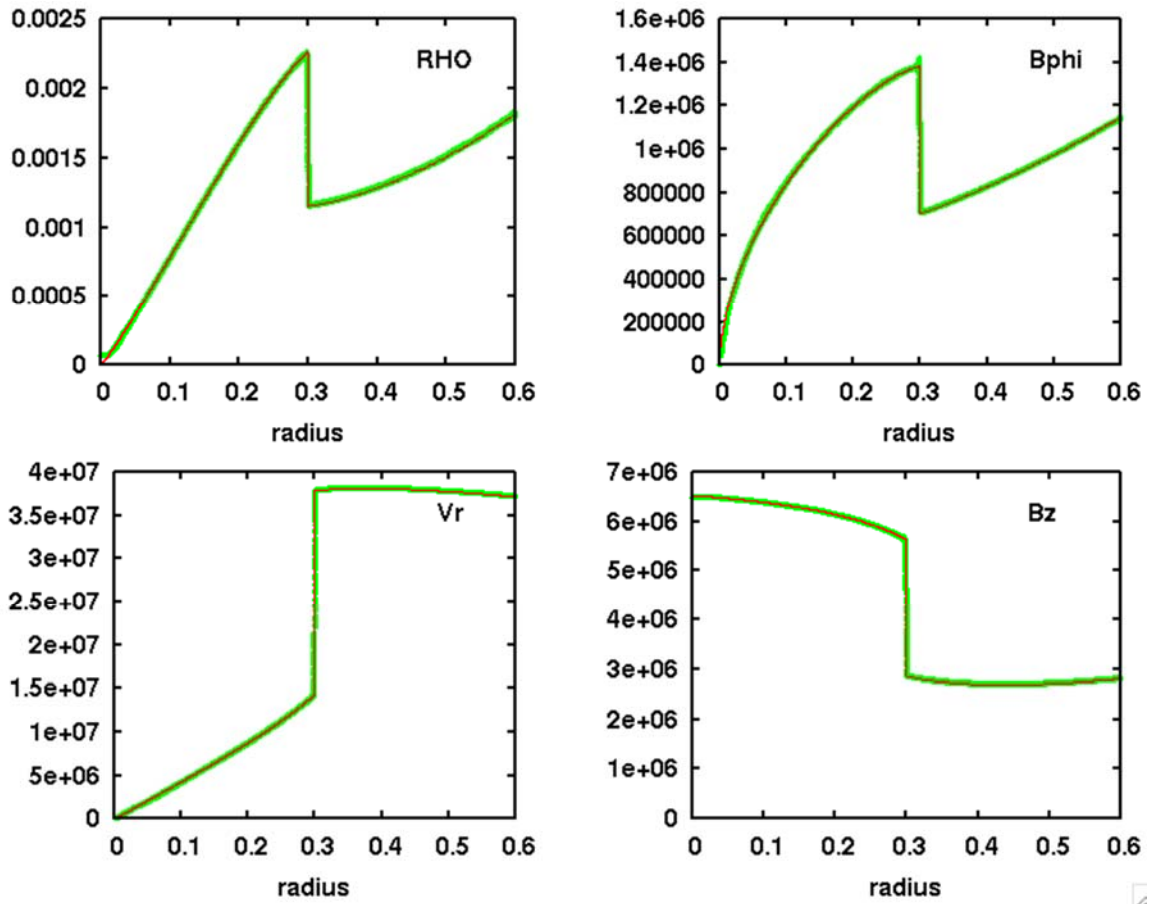
(b)

Figure 10. Problem 2 FLAG box-grid at (a) coarse resolution and (b) under mesh refinement suggesting convergence. Numerical artifact exists on axis, including wall heating (See Ref.[4]).



$x_0 = -0.170096$   $y_0 = -0.305806$   $y_2 = -30.5806$

**Figure 11. Problem 2 FLAG Axis2-grid (Cylindrical) results under radial mesh refinement suggest radial convergence. The red profiles are for  $N_{\text{cells}} = 50$ . The green are for  $N_{\text{cells}} = 100$ . The blue profiles are the analytic solutions.**



**Figure 12. Problem 2 ATHENA fixed-grid solution shows excellent agreement with the analytic solution.**

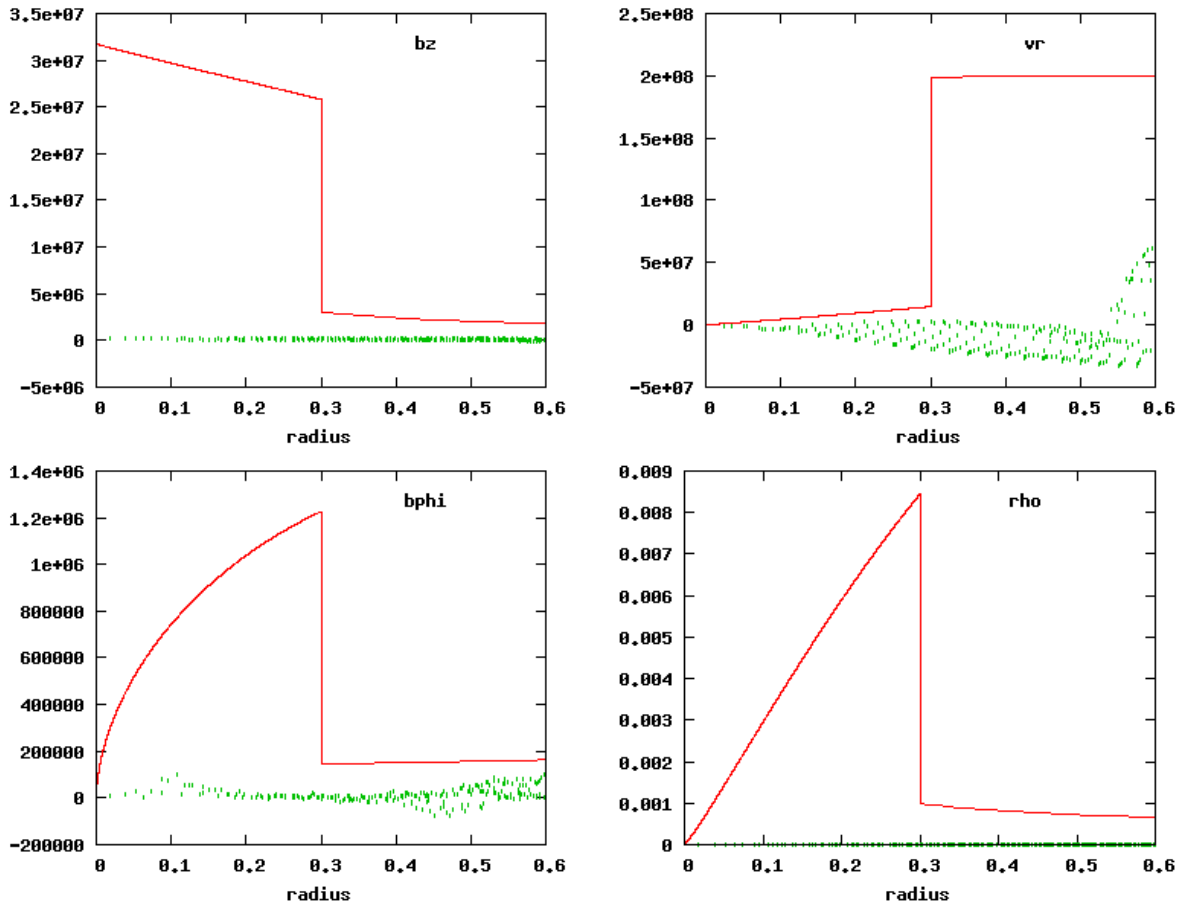


**Figure 13.** Problem 3 FLAG fixed-grid solution does not agree with the analytic solution. The solution was observed to be unstable.

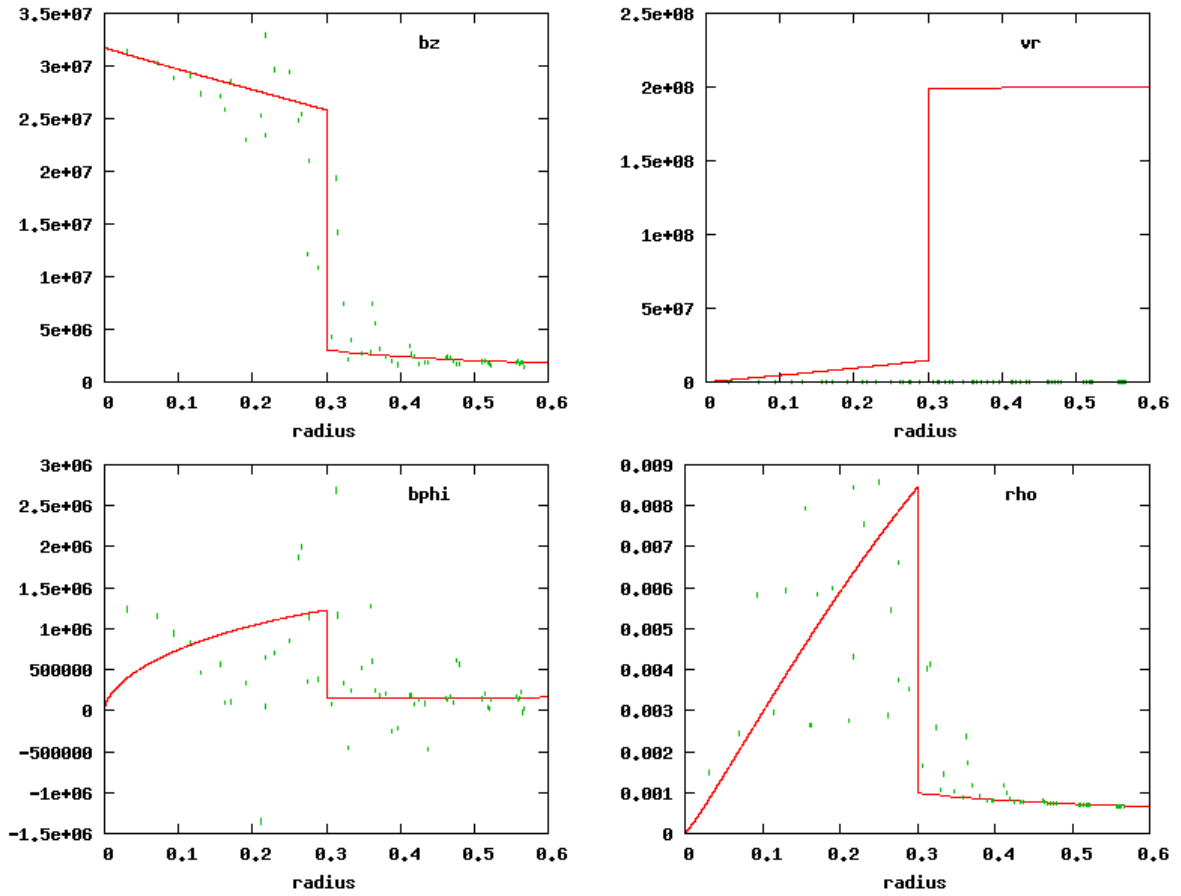


**Figure 14. Problem 3 FLAG box-grid does not agree with the analytic solutions. The solution was observed to be unstable.**

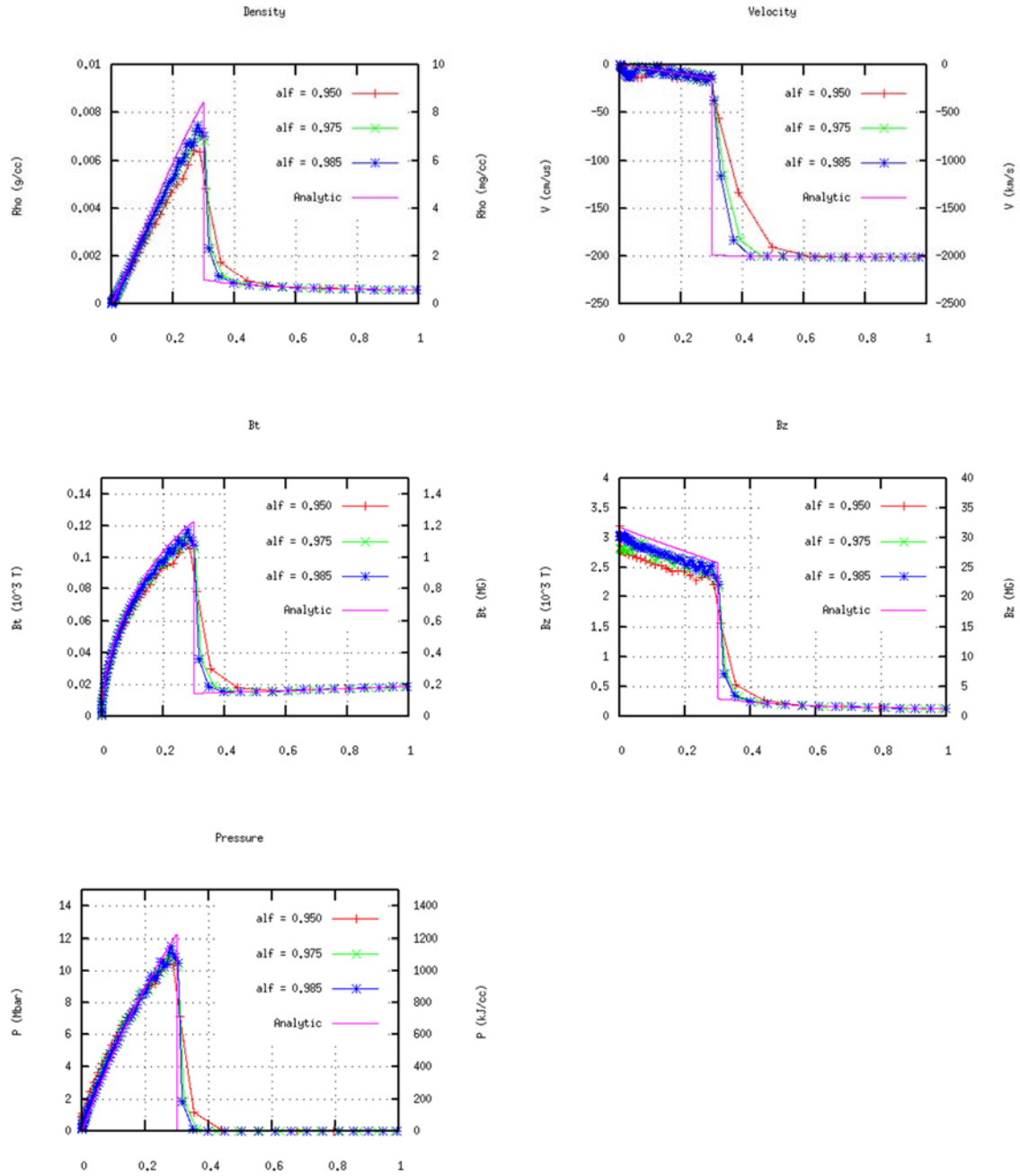
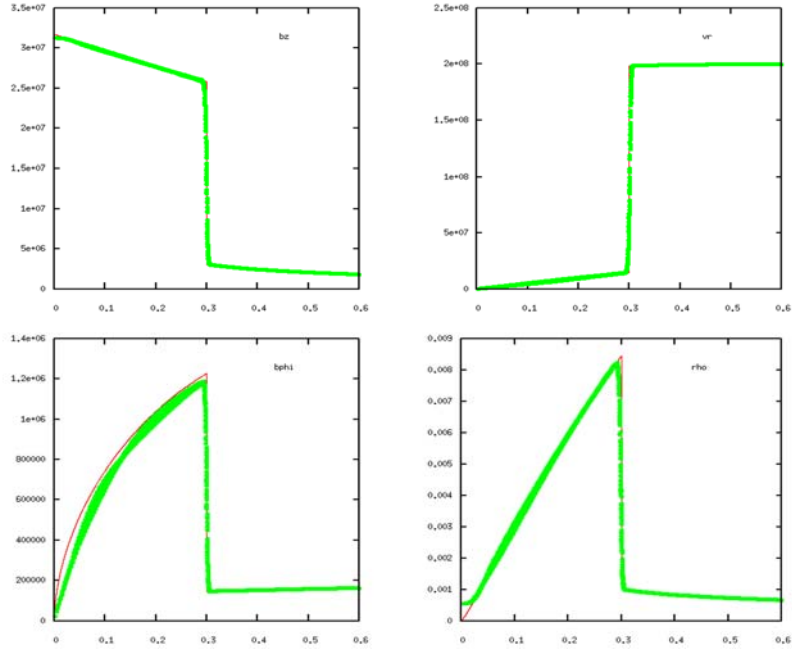
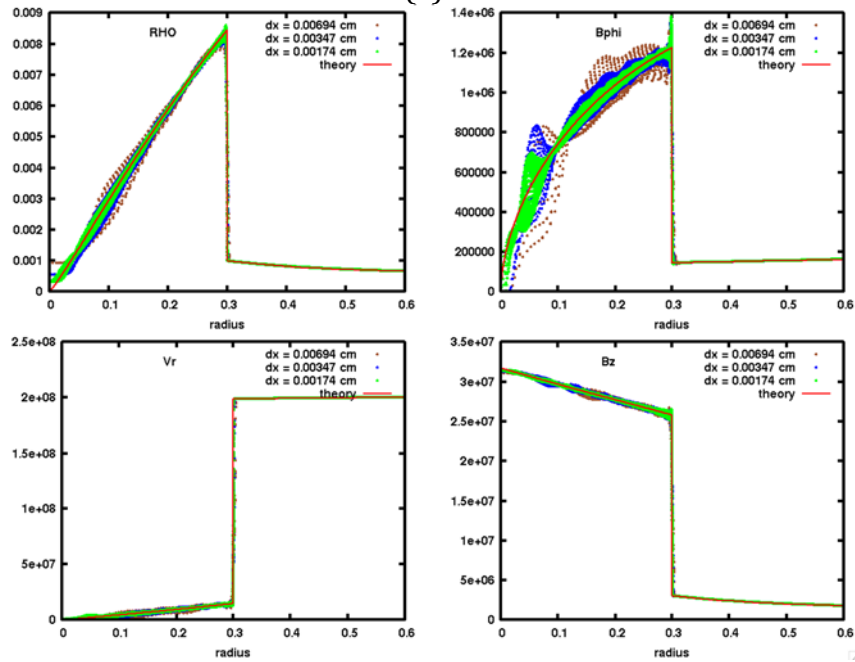


**Figure 15. Problem 3 FLAG axis2-grid (cylindrical) with ratio grid setup. Increasing the parameter,  $0.950 < \alpha < 0.985$ , effectively refines the grid. Nominal convergence to the analytic solution is seen. However, progressively higher mode oscillations behind the shock are also observed with increasing  $\alpha$ , suggesting the potential for instability.**



(a)



(b)

**Figure 16. Problem 3, ATHENA fixed-grid solution for (a) low resolution and (b) under mesh refinement has nominal agreement with analytic solution. Some suggestion of instability exists.**

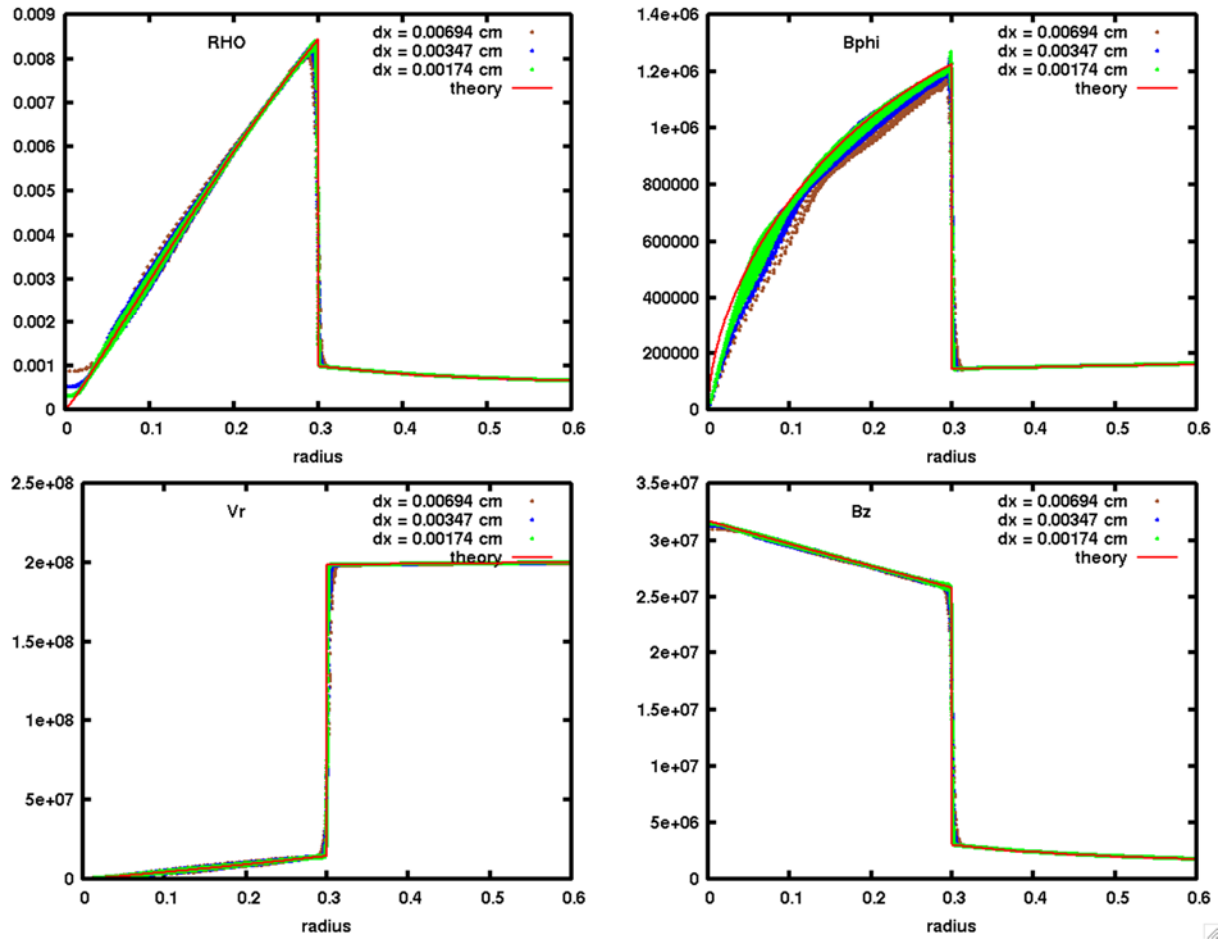


**Figure 17. Problem 3 ATHENA fixed-grid instability is stabilized with grid-scale viscosity and magnetic diffusivity of 2nd order.**